On the multi-dimensional extension of the quincunx subsampling matrix

Dimitri Van De Ville *Member*, Thierry Blu *Member*, Michael Unser *Fellow*

Abstract

The dilation matrix associated with the 3D FCC sublattice is often considered to be the natural 3D extension of the 2D quincunx dilation matrix. However, we demonstrate that both dilation matrices are of different nature: while the 2D quincunx matrix is a similarity transform, the 3D FCC matrix is not. More generally, we show that is impossible to obtain a dilation matrix that is a similarity transform and performs downsampling of the Cartesian lattice by a factor of two in more than two dimensions. Furthermore, we observe that the popular 3D FCC subsampling scheme alternates between three different lattices: Cartesian, FCC, and quincunx. The latter one provides a less isotropic sampling density, a property that should be taken into account to properly orient 3D data before processing using such a subsampling matrix.

Index Terms

Two-channel filterbanks, wavelet decomposition, 2D quincunx sampling, 3D FCC sampling, nonseparable design

D. Van De Ville, T. Blu, M. Unser are with the Biomedical Imaging Group (BIG), Swiss Federal Institute of Technology Lausanne (EPFL), Switzerland.

On the multi-dimensional extension of the quincunx subsampling matrix

I. Introduction

The quincunx sampling scheme is an interesting configuration that is commonly used for designing critically sampled filterbanks and discrete wavelet transforms in 2D [1]–[7]. In contrast to the dyadic separable case, the quincunx dilation matrix leads to a two-channel filterbank architecture—or equivalently one single wavelet—and reduces the scale more progressively: a factor $\sqrt{2}$ instead of 2. We briefly review the 2D quincunx scheme in Sect. II.

The growing availability of 3D volumetric and spatio-temporal data increases the interest for 3D two-channel designs. The dilation matrix associated to the 3D face-centered cubic (FCC) sublattice is often proposed as the natural extension of the 2D quincunx case [7]–[9]. However, we point out a fundamental difference between the 2D quincunx and the 3D FCC matrices: the 3D FCC matrix does not correspond to a similarity transform (i.e., an angle-preservation transformation such as rotation or symmetry combined with dilation) as does the 2D quincunx matrix. Moreover, we show that, for more than two dimensions, it impossible to find a dilation matrix on the Cartesian lattice that is a similarity transform and at the same time leads to a two-channel filterbank. Consequently, when the 3D FCC dilation matrix is cascaded, the Voronoi cells of the sublattices are not just obtained by a simple rotation/symmetry and dilation. In particular, for the 3D FCC case, we observe an alternation between three types of lattices: Cartesian, FCC, and quincunx in the x-z plane. This observation can be useful to guide the orientation of the 3D data before processing. These results are discussed in Sect III.

II. 2D Quincunx Subsampling

We characterize the Cartesian lattice by its sites $\mathbf{k} = [k_1 \ k_2]^{\mathrm{T}}$, $k_1, k_2 \in \mathbb{Z}$. An admissible 2×2 dilation matrix $\mathbf{D}$, mapping $\mathbf{k}$ to $\mathbf{Dk}$, must satisfy the following properties [10], [11]:

1) The new lattice forms a sublattice of the Cartesian lattice; a trivial property when each element of $\mathbf{D}$ is integer.
2) The magnitude of each eigenvalue λ_i of $\mathbf{D}$ must be strictly larger than 1 to ensure a dilation in each dimension.

After applying the dilation matrix, the density of the lattices sites is reduced by a factor $|\det \mathbf{D}|$. The Voronoi cell of the lattice is defined as the set of points closer to the origin than to any other lattice site, and completely characterizes the lattice's geometric structure [12]. The dual or reciprocal lattice is characterized by the matrix which is the transpose of the inverse dilation matrix; the reciprocal lattice serves in the frequency domain to replicate the spectrum while its Voronoi cell can be considered as the Nyquist region [8], [13].

The quincunx sublattice consists of those lattices sites $[k_1\ k_2]^{\mathrm{T}}$, where $k_1 + k_2 = 2n$, n integer. There are two common choices for the corresponding dilation matrix:

$$\mathbf{D}_1 = \begin{bmatrix} 1 & 1 \\ 1 & -1 \end{bmatrix}, \quad \mathbf{D}_2 = \begin{bmatrix} 1 & -1 \\ 1 & 1 \end{bmatrix}. \tag{1}$$

Note that both matrices correspond to a similarity transform; i.e., a symmetry ($\mathbf{D}_1$) or a rotation ($\mathbf{D}_2$), combined with a dilation that reduces the number of sites by a factor of two ($|\det \mathbf{D}_1| = |\det \mathbf{D}_2| = 2$). For signal processing applications, an interesting property is to have the iterated sublattice coincide again with a dilated Cartesian lattice after a few iterations. This property also contributes to the construction of smooth wavelets [14]. For these examples, we have $\mathbf{D}_1^2 = 2\mathbf{I}$ and $\mathbf{D}_2^8 = 16\mathbf{I}$.

The design of orthogonal filters for quincunx sampling is strongly determined by the shape of the Voronoi cell of the reciprocal sampling lattice. More specifically, the goal is to design an orthogonal filter whose frequency response is reasonably close to the ideal filter characterized by the indicator function of the Nyquist region of the sampling lattice in the frequency domain, which correspond to the Voronoi cell of the reciprocal lattice. Some filter and wavelet design examples can be found in [5], [7], [10], [15]–[19].

Since the 2D quincunx matrix corresponds to a similarity transform, its associated Voronoi cell in the spatial and the frequency domain is simply rotated or mirrored and dilated. Therefore, iterating $\mathbf{D}_1$ and $\mathbf{D}_2$ alternates between a Cartesian and a quincunx sublattice.

III. 3D FCC Subsampling

The dilation matrix corresponding to the 3D FCC sublattice is often considered to be the natural extension of the 2D quincunx scheme. The corresponding most popular dilation matrix (cf. [4], [8], [10], [20]) is

$$\mathbf{D} = \begin{bmatrix} 1 & 0 & 1 \\ -1 & -1 & 1 \\ 0 & -1 & 0 \end{bmatrix}. \tag{2}$$

It leads to a two-channel design ($|\det \mathbf{D}| = 2$) and coincides with a dilated Cartesian lattice after three iterations; i.e., we have $\mathbf{D}^3 = 2\mathbf{I}$.

The use of the FCC sampling scheme is motivated by the energy packing argument [21]. Indeed, together with the body-centered cubic (BCC) lattice, the FCC lattice has the densest lattice packing in 3D: it retains a maximal energy proportion for signals with a spherical spectrum[1]. Therefore, as in the 2D case, the shape of the frequency response of an orthogonally designed filter on the FCC lattice tends to the indicator function of the Voronoi cell of the BCC lattice, which is a space-filling polyhedron that fills the space in an optimal way for signals with a spherical spectrum. Some examples of 3D filter design can be found in [10], [17], [19], [20], [22]–[24].

However, there is a fundamental difference between the 2D quincunx and the 3D FCC dilation matrix. The latter does not correspond to a similarity transform. More generally, we can show the following.

[1]In signal processing literature, the term face-centered orthorhombic (FCO) is often used instead of FCC. However, the FCO lattice allows for a scaling along the coordinate axes and therefore the argument of maximal energy compaction for signals with a spherical spectrum is no longer valid. Since the scaling is rarely used, we prefer he use of the term FCC.

Proposition 1: For dimensions greater than 2, no dilation matrix can be a similarity matrix with determinant 2.

Proof: Assume that $\mathbf{D}$ is an admissable dilation matrix in N dimensions that corresponds to a similarity transform. Then it should satisfy

$$\mathbf{D}^{\mathrm{T}}\mathbf{D} = m\mathbf{I}, \tag{3}$$

where m is an integer. Taking the determinant of (3) gives

$$|\det \mathbf{D}| = \sqrt{m^N}. \tag{4}$$

On the other hand, by the two-channel design constraint, we need

$$|\det \mathbf{D}| = 2. \tag{5}$$

Satisfying both constraints (4) and (5) would require

$$m = \sqrt[N]{4}, \tag{6}$$

with m integer, which is only possible for $N = 2$. ■

Now we know that no 3D dilation matrix with determinant 2 exists that corresponds to a similarity transform. Nevertheless, it is interesting to take a closer look at the popular 3D FCC matrix (2) and the consequences of not having this property. For this purpose, we determine the Voronoi cell at each iteration for both the spatial and the dual lattice [12], [21]. Since we have $\mathbf{D}^3 = 2\mathbf{I}$, the iterated scheme alternates between three lattices, but due to the lack of being a similarity transform, with fundamentally different Voronoi cells. For $\mathbf{D}^{3n}$, $n \in \mathbb{N}$, we have the Cartesian lattice and the corresponding cubic Voronoi cell in the spatial and the frequency domain, see Fig. 1 (a) and (b). For $\mathbf{D}^{3n+1}$, we have the FCC lattice in the spatial domain (Fig. 1 (c)) where the Voronoi cell is a rhombic dodecahedron, and the BCC lattice in the frequency domain (Fig. 1 (d)) where the Voronoi cell is a truncated octahedron. Finally, for $\mathbf{D}^{3n+2}$, we obtain a quincunx sublattice in the x-z plane, while the y dimension is already subsampled by 2; see Fig. 1 (e) and (f), respectively. Logically, the Voronoi cell of the spatial domain gets larger when the lattice gets coarser, while the inverse happens for the dual lattice. The lattices are also illustrated by 2D cuts in Fig. 2. The alternation between those lattices is summarized in Table I and has two important consequences. First, the optimal energy packing argument for orthogonal filter design is only valid for one of the three lattices. Second, the quincunx arrangement for each third lattice $\mathbf{D}^{3n+2}$ has a less isotropic sampling density, which also influences orthogonally designed filters. Applications can use this property to properly adapt the orientation of 3D data before treatment; e.g., for spatio-temporal data, the temporal direction could be put along the y-axis.

IV. Conclusion

The 3D FCC dilation matrix is often considered to be the natural extension of the 2D quincunx case. However, the dilation matrices have a different nature. In this paper, we have shown that the popular 3D FCC dilation matrix, as opposed to the 2D quincunx matrix, does not correspond to a similarity transform. Moreover, for more than two dimensions, it is impossible to build a two-channel dilation matrix on the Cartesian lattice which

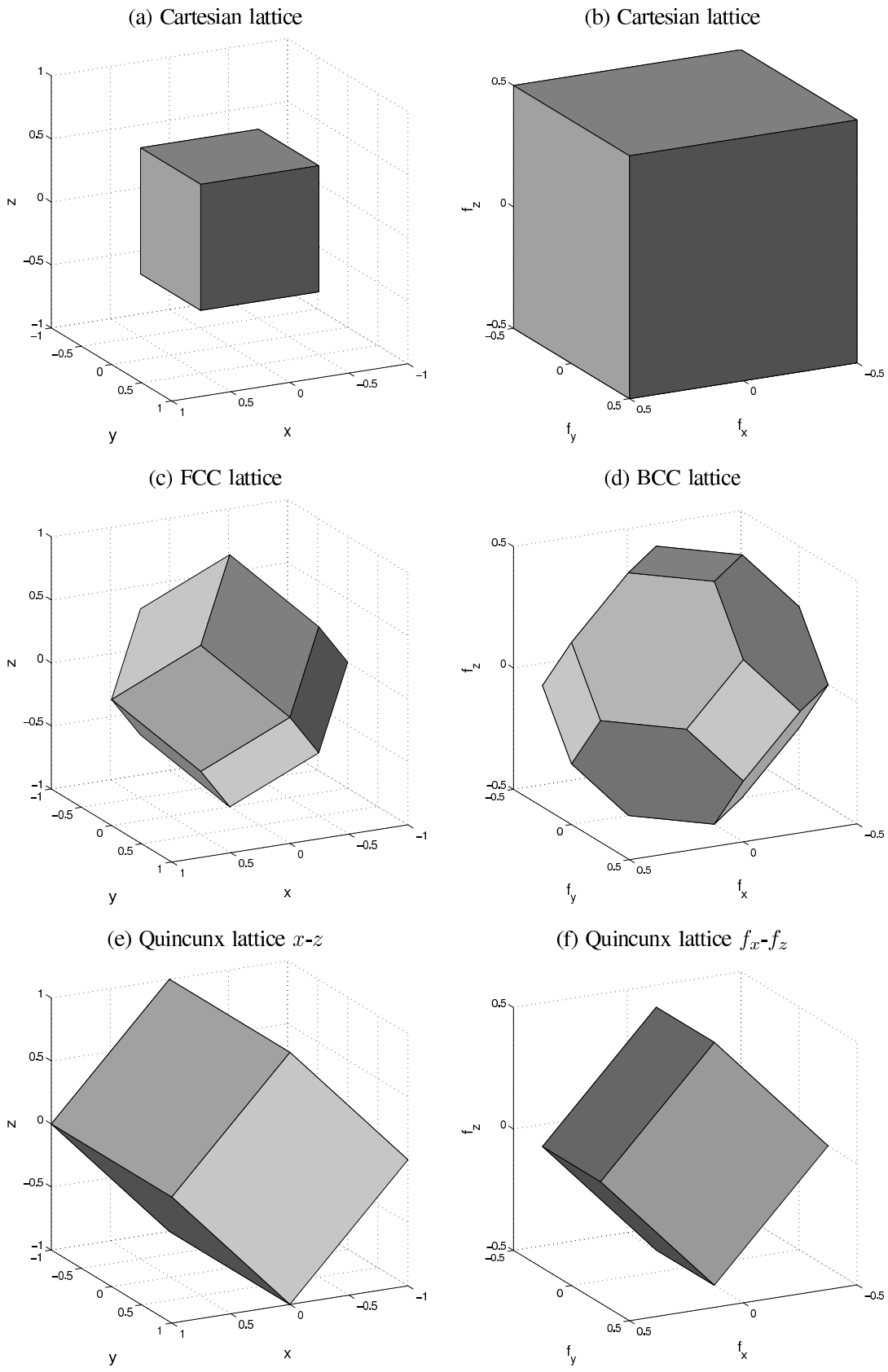

Fig. 1. Types of 3D lattices encountered when the 3D FCC dilation matrix is iterated. At the left side: the Voronoi cell of the lattice in the spatial domain for the lattices (a) $\mathbf{D}^0\mathbf{k}$, (c) $\mathbf{D}^1\mathbf{k}$, (e) $\mathbf{D}^2\mathbf{k}$ (notice that the side in the x-z plane have length $\sqrt{2}$, while the sides in the y direction have length 2). At the right side: the Voronoi cell of the reciprocal lattice in the frequency domain for the lattices (b) $(\mathbf{D}^{-\mathrm{T}})^0\mathbf{k}$, (d) $(\mathbf{D}^{-\mathrm{T}})^1\mathbf{k}$, (f) $(\mathbf{D}^{-\mathrm{T}})^2\mathbf{k}$.

TABLE I

PROPERTIES OF THE ITERATED 3D FCC MATRIX OF (2).

iteration	spatial lattice	reciprocal lattice	sampling density
$3n$	Cartesian lattice	Cartesian lattice	$2^{3n}(1,1,1)$
$3n+1$	FCC lattice	BCC lattice	$2^{3n}(\sqrt[3]{2}, \sqrt[3]{2}, \sqrt[3]{2})$
$3n+2$	Quincunx (x-z)	Quincunx (f_x-f_z)	$2^{3n}(\sqrt{2}, 2, \sqrt{2})$

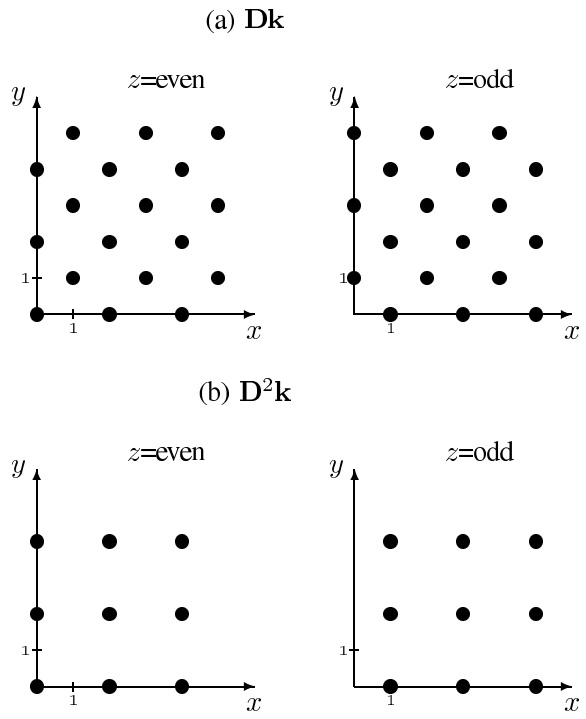

Fig. 2. 2D cuts of the 3D lattices obtained by iterating the 3D FCC dilation. (a) $\mathbf{Dk}$. (b) $\mathbf{D^2k}$.

corresponds to a similarity transform. Still, the 3D FCC dilation matrix can be useful to treat 3D volumetric or spatiotemporal data. However, one should be aware that iterating the dilation matrix produces an alternation between lattices with a different degree of isotropy; i.e., Cartesian, FCC, and quincunx lattices.

REFERENCES

[1] M. Vetterli, "Multi-dimensional sub-band coding: Some theory and algorithms," *Signal Processing*, vol. 6, no. 2, pp. 97–112, Feb. 1984.

[2] R. Ansari, H. Gaggioni, and D. J. LeGall, "HDTV coding using a non-rectangular subband decomposition," in *Proc. SPIE Conf. Vis. Commun. Image Processing*, Cambridge, MA, 1988, pp. 821–824.

[3] J.-C. Feauveau, *Analyse multirésolution par ondelettes non orthogonales et bancs de filtres numériques*, Ph.D. thesis, Univ. Paris Sud, 1990.

[4] M. Vetterli, J. Kovačević, and D. J. LeGall, "Perfect reconstruction FIR filter banks: some properties and factorizations," *Image Commun.*, vol. 2, no. 3, pp. 349–364, Oct. 1990.

[5] E. Viscito and J. P. Allebach, "The analysis and design of multidimensional FIR perfect reconstruction filter banks for arbitrary sampling lattices," *IEEE Transactions on Circuits and Systems*, vol. 38, no. 1, pp. 29–42, Jan. 1991.

[6] A. Cohen and I. Daubechies, "Non-separable bidimensional wavelet bases," *Revista Matematica Iberoamericana*, vol. 9, pp. 51–137, 1993.

[7] J. Kovačević and W. Sweldens, "Wavelet families of increasing order in arbitrary dimensions," *IEEE Transactions on Image Processing*, vol. 9, no. 3, pp. 480–496, Mar. 2000.

[8] E. Dubois, "The sampling and reconstruction of time-varying imagery with application in video systems," *Proceedings of the IEEE*, vol. 73, no. 4, pp. 502–522, Apr. 1985.

[9] P. Dafas, I. Kompatsiaris, and M. G. Strintzis, *Advances in Geometric Modeling*, chapter Optimal Hierarchical Adaptive Mesh Construction Using FCO Sampling, Wiley Europe, Dec. 2003.

[10] J. Kovačević and M. Vetterli, "Nonseparable multidimensional perfect reconstruction filter banks and wavelet bases for $\mathbb{R}^n$," *IEEE Transactions on Information Theory*, vol. 38, no. 2, pp. 533–555, Mar. 1992.

[11] K. Gröchenig and W. R. Madych, "Multiresolution analysis, Haar bases and self-similar tilings of $\mathbb{R}^n$," *IEEE Transactions on Information Theory*, vol. 38, pp. 556–568, Mar. 1992.

[12] E. Viberbo and E. Biglieri, "Computing the Voronoi cell of a lattice: The diamond-cutting algorithm," *IEEE Transactions on Information Theory*, vol. 42, no. 1, pp. 161–171, Jan. 1996.

[13] D. P. Petersen and D. Middleton, "Sampling and reconstruction of wave-number-limited functions in N-dimensional Euclidean spaces," *Information and control*, vol. 5, pp. 279–323, 1962.

[14] K. Gröchenig and A. Ron, "Tight compactly supported wavelet frames of arbitrarily high regularity," *Proc. Amer. Math. Soc.*, , no. 126, pp. 1101–1107, 1998.

[15] R. H. Bamberger and M. J. T. Smith, "A filter bank for the directional decomposition of images: Theory and design," *IEEE Transactions on Signal Processing*, vol. 40, no. 4, pp. 882–893, Apr. 1992.

[16] T. Chen and P. P. Vaidyanathan, "Multidimensional multirate filters and filter banks derived from one-dimensional filters," *IEEE Transactions on Signal Processing*, vol. 41, no. 5, pp. 1749–1765, May 1993.

[17] J. Kovačević and M. Vetterli, "Nonseparable two- and three-dimensional wavelets," *IEEE Transactions on Signal Processing*, vol. 43, no. 5, pp. 1269–1273, 1995.

[18] K. S. C. Pun and T. Q. Nguyen, "A novel and efficient design of multidimensional PR two-channel filter banks with hourglass-shaped passband support," *IEEE Signal Processing Letters*, vol. 11, no. 3, pp. 345–348, Mar. 2004.

[19] M. Feilner, D. Van De Ville, and M. Unser, "An orthogonal family of quincunx wavelets with continuously-adjustable order," *IEEE Transactions on Image Processing*, 2004, in press.

[20] J. Kovačević and M. Vetterli, "FCO sampling of digital video using perfect reconstruction filter banks," *IEEE Transactions on Image Processing*, vol. 2, no. 1, pp. 118–122, 1993.

[21] J. H. Conway and N. J. A. Sloane, *Sphere Packings, Lattices, and Groups*, Springer-Verlag, New York, 2nd edition, 1993.

[22] D. B. H. Tay and N. G. Kingsbury, "Design of nonseparable 3-D filter banks/wavelet bases using transformations of variables," *IEE Proc.-Vis. Image Signal Process.*, vol. 143, no. 1, pp. 51–61, Feb. 1996.

[23] D. B. H. Tay, "Analytical design of 3-D wavelet filter banks using the multivariate Bernstein polynomial," *IEE Proc.-Vis. Image Signal Process.*, vol. 147, no. 2, pp. 122–130, Apr. 2000.

[24] D. B. H. Tay, "Parametric Bernstein polynomial for least squares design of 3-D wavelet filter banks," *IEEE Transactions on Circuits and Systems–I: Fundamental Theory and Applications*, vol. 49, no. 6, pp. 887–891, June 2002.